Catalysis Today 166 (2011) 135–139

Contents lists available at ScienceDirect

Catalysis Today

journal homepage: www.elsevier.com/locate/cattod

Photocatalytic degradation of methyl orange using Bi_2MNbO_7 (M = Al, Fe, Ga, In) semiconductor films on stainless steel

K.L. Rosas-Barrera[a], J.L. Ropero-Vega[b], J.A. Pedraza-Avella[b], M.E. Niño-Gomez[b], J.E. Pedraza-Rosas[a], D.A. Laverde-Cataño[a,*]

[a] Grupo de Investigaciones en Minerales, Biohidrometalurgia y Ambiente – GIMBA, Universidad Industrial de Santander – UIS, Sede Guatiguará, Km. 2 vía El Refugio, C.P. 681011, Piedecuesta (Santander), Colombia
[b] Centro de Investigaciones en Catálisis – CICAT, Universidad Industrial de Santander – UIS, Sede Guatiguará, Km. 2 vía El Refugio, C.P. 681011, Piedecuesta (Santander), Colombia

ARTICLE INFO

Article history:
Available online 22 September 2010

Keywords:
Sol–gel method
Dip-coating technique
Pyrochlore-type structure
Photocatalytic oxidation
Photodegradation of dyes

ABSTRACT

Semiconductor Bi_2MNbO_7 (M = Al, Fe, Ga, In) films on AISI/SAE 304 stainless steel were prepared by sol–gel dip-coating followed by a thermal treatment at 500 °C. The films were made by depositing different number of layers (1, 3 and 5) at different withdrawal speeds (5.0, 7.5 and 10.0 cm/min). They were characterized by X-ray diffraction, scanning electron microscopy and energy dispersive X-ray fluorescence. The photocatalytic activity of Bi_2MNbO_7 films was evaluated by the degradation of methyl orange. The photodegradation kinetics was investigated and compared with those of TiO_2 films prepared by a similar procedure. The films exhibited the following photocatalytic performance: $Bi_2GaNbO_7 > Bi_2FeNbO_7 > Bi_2AlNbO_7 > TiO_2 \geq Bi_2InNbO_7 \gg$ UV light. It is worth noting that the photoactivity of Bi_2MNbO_7 films toward methyl orange degradation was higher or equivalent than that of TiO_2 films.

1. Introduction

In the last decade, the so-called Advanced Oxidation Processes (AOPs) have been proposed as alternative methods for water purification [1,2]. Among AOPs, heterogeneous photocatalysis appears as an emerging destructive technology leading to the total mineralization of most of the organic pollutants [3–5].

Titanium dioxide suspensions have been widely used for the degradation of many compounds due to its exceptional optical and electronic properties, chemical stability, non-toxicity and low cost [6,7]. However, this typical photocatalyst has some disadvantages such as the need of UV light excitation and the difficulty of recovering it completely after the treatment process.

For those reasons, the search of new promising photocatalysts which will be able to operate with visible light [8–10] and their immobilization on inert supports [11–13] are important challenges to extend the range of such applications. The sol–gel method, by dip- and spin-coating techniques, constitutes one of the simplest and promising approaches for synthesizing new film materials with controlled optical, structural and morphological properties [14–16].

In this sense, a new series of photocatalysts, Bi_2MNbO_7 (M = Al, Fe, Ga, In, Sm), were synthesized as powders, by a solid–state reaction [17] and a sol–gel process [18], and recently as thin films on glass slides, by sol–gel dip-coating [19].

In the present study, the photocatalytic activity of dip-coating films of Bi_2MNbO_7 (M = Al, Fe, Ga, In) on AISI/SAE 304 stainless steel, with different number of layers at different withdrawal speeds, was evaluated by the degradation of methyl orange (Fig. 1), which was used as a model compound [20–25].

2. Experimental

2.1. Materials

The following reagents were used as received without further purification: bismuth(III) acetate (Aldrich, 99.99%), aluminum(III) acetylacetonate (Aldrich, 99.999%), gallium(III) acetylacetonate (Aldrich, 99.99%), indium(III) acetylacetonate (Aldrich, 99.99%), iron(III) acetylacetonate (Aldrich, 99.9%), niobium(V) ethoxide (Aldrich, 99.95%), titanium(IV) isopropoxide (Aldrich, 97%), 2-propanol (Merck, 99.5%), ethanol (Merck, 99.9%), acetylacetone (Aldrich, 99%), HNO_3 (Carlo

* Corresponding author. Tel.: +57 7 6550802; fax: +57 7 6550802.
E-mail addresses: apedraza@uis.edu.co (J.A. Pedraza-Avella), dlaverde@uis.edu.co (D.A. Laverde-Cataño).

0920-5861/$ – see front matter © 2010 Elsevier B.V. All rights reserved.
doi:10.1016/j.cattod.2010.08.008

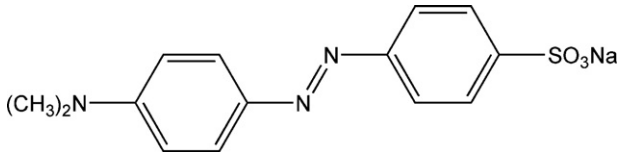

Fig. 1. Molecular structure of MeO.

Erba, 65%), methyl orange (Merck, 100%) and distilled water (1 MΩ cm).

2.2. Preparation of the films

Semiconductor films of Bi–M–Nb–O (M = Al, Fe, Ga, In) system were prepared by dip-coating on AISI/SAE 304 stainless steel (304 SS) plates (15 mm × 25 mm), which were ultrasonically cleaned in ethanol (15 min) prior to use. Details of the sol preparation were described elsewhere [19]. The films were made by depositing different number of layers (1, 3 and 5) at different withdrawal speeds (5.0, 7.5 and 10.0 cm/min). They were dried at room temperature (25 °C) for 1 h after each layer deposition and finally annealed at 500 °C for 4 h.

TiO_2 films were also prepared by a similar procedure for comparative purposes [26].

2.3. Characterization of the films

Scanning electron microscopy (SEM) micrographs were obtained with a LEO 430 microscope operated at 20 kV in secondary electron mode.

X-ray diffraction (XRD) patterns were collected on a PANalytical X'Pert PRO diffractometer operated at 40 kV and 40 mA, using Cu Kα radiation (λ = 1.540598 Å) selected with Ni filter, in the thin film mode with a step of 0.02° and a counting time of 1.0 s per step.

Elemental analyses were performed by energy dispersive X-ray fluorescence (EDXRF) in a Shimadzu EDX-800HS spectrometer equipped with a Rh tube and a Si(Li) detector. The measurements were performed in vacuum atmosphere and the quantification was performed using fundamental parameters method.

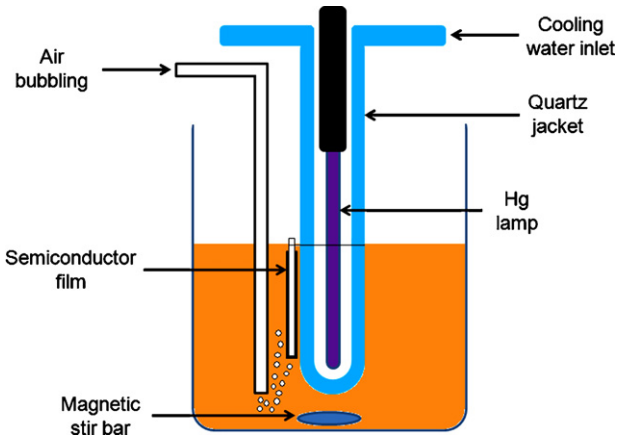

Fig. 2. Schematic representation of the photoreactor.

2.4. Photocatalytic evaluation of the films

The photocatalytic activity of the Bi_2MNbO_7 (M = Al, Fe, Ga, In) films on 304 SS was evaluated by the degradation of methyl orange (MeO). A 200 mL glass cell equipped with an immersion Hg lamp (UVP Pen-Ray 5.5 W) was employed in the photocatalytic experiments (Fig. 2). In all tests, 40 mL of aqueous solution containing 5 ppm of MeO were used at natural pH. Before starting each test, the system was kept in the dark for 15 min to achieve the adsorption equilibrium. The reaction was carried out during 2 h with continuous air bubbling and magnetic stirring. Samples were taken each 30 min and the MeO concentration was determined by colorimetry, using the 460 nm absorption band, in a LaMotte Smart apparatus. The reaction also was carried out using TiO_2 films on 304 SS as reference. Blank reaction was done without semiconductor films in order to determine the contribution of photolytic degradation.

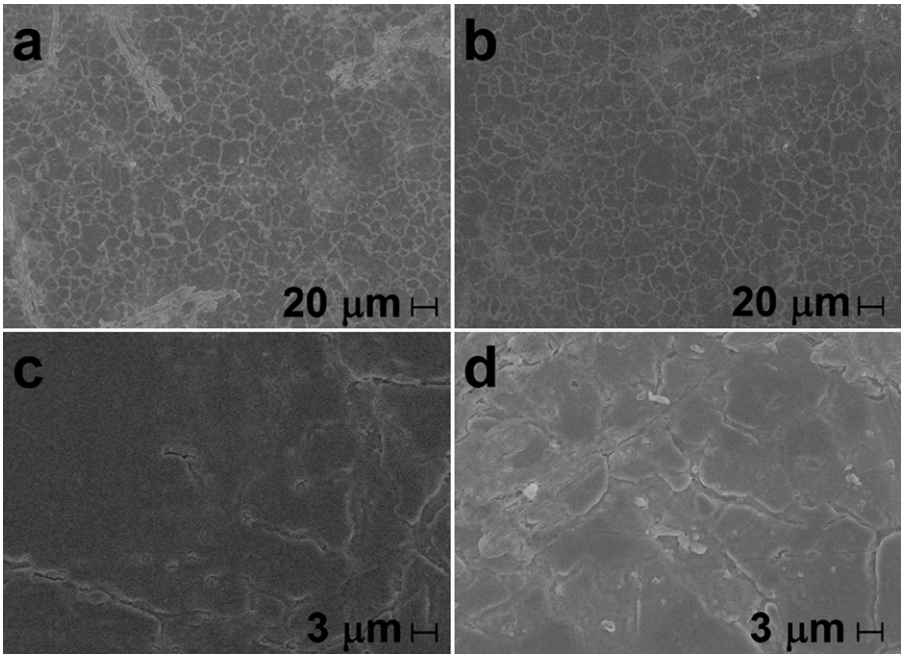

Fig. 3. SEM micrographs of Bi_2GaNbO_7 films on 304 SS: (a) 1 layer at 5.0 cm/min (1000×), (b) 1 layer at 7.5 cm/min (1000×), (c) 3 layers at 5.0 cm/min (7000×), (d) 3 layers at 7.5 cm/min (7000×).

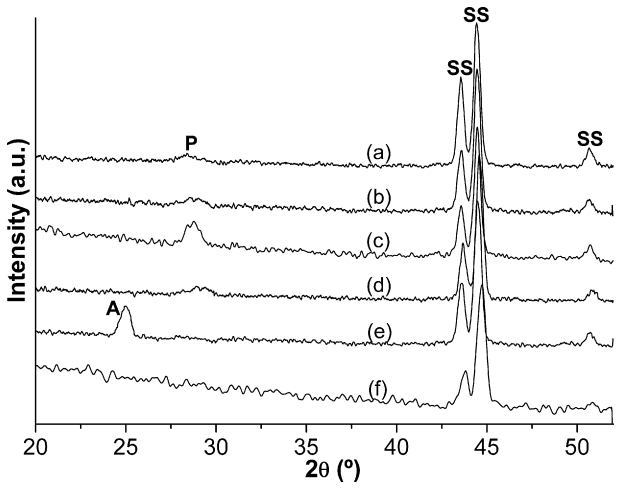

Fig. 4. XRD patterns of (a) Bi_2AlNbO_7, (b) Bi_2FeNbO_7, (c) Bi_2GaNbO_7, (d) Bi_2InNbO_7 and (e) TiO_2 films on 304 SS (3 layers at 7.5 cm/min) and (f) 304 SS annealed at 500 °C.

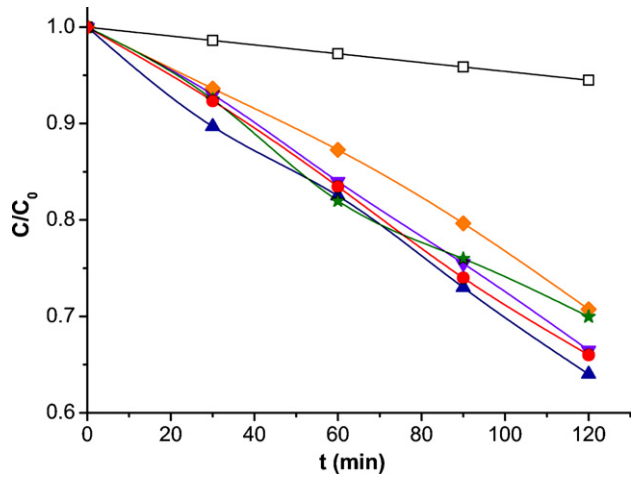

Fig. 5. Relative concentration of MeO vs. time using: (▼) Bi_2AlNbO_7, (●) Bi_2FeNbO_7, (▲) Bi_2GaNbO_7, (♦) Bi_2InNbO_7 and (⋆) TiO_2 films on 304 SS (3 layers at 7.5 cm/min) and (□) UV light (without photocatalyst).

3. Results and discussion

3.1. Scanning electron microscopy

SEM micrograph of Bi_2GaNbO_7 film (1 layer) on 304 SS obtained at 5.0 cm/min show a fairly flat but cracked surface (Fig. 3a). The formation of microcracks all over the surface may be a consequence of the coating contraction during the heat treatment [27]. When the withdrawal speed was increased to 7.5 cm/min, the cracks became slightly thinner (Fig. 3b) probably because the thickness of the films increased.

When the number of layers was increased to 3, the cracks were covered partially but agglomerates appeared (Fig. 3c and d) because the amount of deposited material increased.

3.2. X-ray diffraction

XRD patterns of Bi_2MNbO_7 (M = Al, Fe, Ga, In) films on 304 SS (3 layers at 7.5 cm/min) are shown in Fig. 4. Only broad peaks at about 28.7° corresponding to the pyrochlore structure-type could be identified [28]. The peaks present at 43.6, 44.6 and 50.7° correspond to the stainless steel support [29]. It is strongly proposed that such a broad peaks are due to the low amount of deposited material (about 8 mg by layer), the small crystallite size and the poor crystallinity [30]. Although the Bi_2MNbO_7 films showed similar XRD patterns, the 2θ angles of the pyrochlore reflection were slightly different: Bi_2AlNbO_7 (28.37°) < Bi_2FeNbO_7 (28.63°) < Bi_2GaNbO_7 (28.77°) < Bi_2InNbO_7 (28.97°). They were shifted according to the ionic radius of the 6-coordinated substituent atom M^{3+}: Al (67.5 pm) < Fe (69 pm) < Ga (76 pm) < In (94 pm) [31]. It is worth noting that the (1 0 1) anatase reflection at 25.11° in the XRD pattern of the TiO_2 film (Fig. 4e) is more intense that the corresponding pyrochlore reflections indicating that the latter material is more crystalline.

Table 1
Elemental analysis of the Bi_2MNbO_7 (M = Al, Fe, Ga, In) films (3 layers at 7.5 cm/min) on 304 SS.

Film	Bi (at.%)	M (at.%)	Nb (at.%)
Bi_2AlNbO_7	70.3	16.1	13.6
Bi_2FeNbO_7	64.8	19.1	16.1
Bi_2GaNbO_7	54.5	23.1	22.4
Bi_2InNbO_7	76.7	12.6	10.7
Bi_2MNbO_7[a]	50.0	25.0	25.0

[a] Stoichiometric ratio.

3.3. Energy dispersive X-ray fluorescence

EDXRF results of Bi_2MNbO_7 (M = Al, Fe, Ga, In) films (3 layers at 7.5 cm/min) on 304 SS are summarized in Table 1. Elemental analyses indicate that the atomic percentages of Bi–Ga–Nb–O sample fit better to the stoichiometric ratio of pyrochlore-type structure (Bi_2MNbO_7). In the other samples an excess of Bi was detected suggesting the presence of $Bi_5Nb_3O_{15}$ [18], $Bi_5In_2Nb_3O_{18-x}$ [32] or Bi_2O_3/Bi_2O_{4-x} [33].

3.4. Photodegradation of methyl orange

MeO degradation over time using Bi_2MNbO_7 (M = Al, Fe, Ga, In) and TiO_2 films on 304 SS (3 layers at 7.5 cm/min) is shown in Fig. 5. It can be seen that the films exhibit the following photocatalytic performance: $Bi_2GaNbO_7 > Bi_2FeNbO_7 > Bi_2AlNbO_7 > TiO_2 \geq Bi_2InNbO_7 \gg$ UV light. Slight differences between the films with different substituent atom M were detected. These can be correlated to their stoichiometric deviations in regard to Bi_2MNbO_7 (see Table 1). Although the photoactivity of Bi_2InNbO_7 is comparable to that of TiO_2 at the end of the test, it is worth noting that the second one tends to decrease with the time. There is a change in the slope at about 60 min. The photocatalytic behavior of Bi_2MNbO_7 films with regard to TiO_2 films could be related to their poor crystallinity (see Fig. 4).

The curves C/C_0 vs. time are well described by a mono-exponential curve suggesting the heterogeneous character of the reaction and that a pseudo-first-order reaction model can be used to describe the kinetic behavior of the films. Using a modified Langmuir–Hinshelwood model, the rate of photodegradation can be expressed as:

$$r = -\frac{dC}{dt} = \frac{k_r K C_0}{1 + K C_0} \quad (1)$$

Due to the low concentration of methyl orange ($KC_0 \ll 1$), the term KC_0 in the denominator could be neglected. Integration of Eq. (1) with initial condition $C = C_0$ at $t = 0$ gives:

$$\ln\left(\frac{C_0}{C}\right) = k_{app} t \quad (2)$$

where $k_{app} = k_r K$ is an apparent first-order rate constant.

Table 2
Kinetic parameters for the MeO photodegradation (2 h) over Bi_2MNbO_7 (M = Al, Fe, Ga, In) films on 304 SS (3 layers at 7.5 cm/min).

Photocatalyst	Apparent first-order rate constant, $k_{app} \times 10^{-3}$ (min^{-1})	Half-life time, $t_{1/2}$ (min)	Correlation coefficient, R^2
UV light	0.47	1475	0.9999
Bi_2AlNbO_7	3.41	203	0.9955
Bi_2FeNbO_7	3.51	197	0.9971
Bi_2GaNbO_7	3.66	189	0.9969
Bi_2InNbO_7	2.85	243	0.9919
TiO_2	3.04	228	0.9970

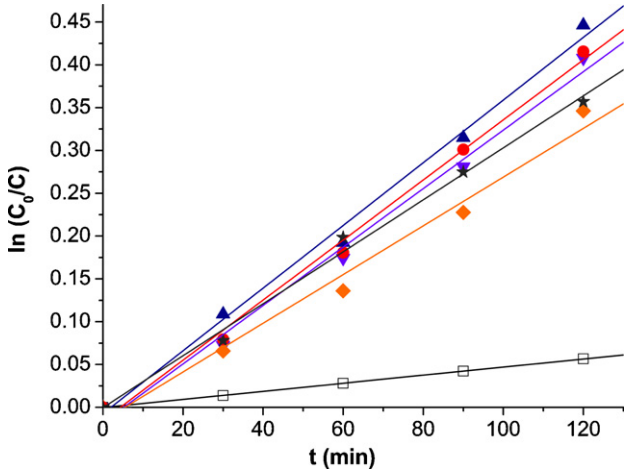

Fig. 6. Linear transformation of the relative concentration of MeO vs. time using: (▼) Bi_2AlNbO_7, (●) Bi_2FeNbO_7, (▲) Bi_2GaNbO_7, (♦) Bi_2InNbO_7 and (★) TiO_2 films on 304 SS (3 layers at 7.5 cm/min) and (□) UV light (without photocatalyst).

The plot of $\ln C_0/C$ vs. t represents a straight line, where k_{app} is the slope of linear regression, and it is shown in Fig. 6.

For a pseudo-first-order reaction, the half-life time ($t_{1/2}$) can be calculated according Eq. (3):

$$t_{1/2} = \frac{\ln 2}{k_{app}} \quad (3)$$

The corresponding values of the kinetic parameters (k_{app}, $t_{1/2}$) for each photocatalyst are shown in Table 2.

All the films showed a higher photocatalytic activity than that obtained with only UV light. The photoactivity of Bi_2MNbO_7 films was higher or equivalent than TiO_2 films. The Bi_2GaNbO_7 film exhibited the highest k_{app} and therefore the lowest $t_{1/2}$. This result can be explained due to the atomic percentages of Bi–Ga–Nb–O sample fit better to the stoichiometric ratio of pyrochlore-type structure (Bi_2MNbO_7) according to the EDXRF results (see Table 1).

MeO degradation over time using Bi_2GaNbO_7 films on 304 SS (3 layers) made at different withdrawal speed (5.0, 7.5 and 10.0 cm/min) is shown in Fig. 7. It can be seen that the degradation increases with a faster withdrawal speed. The highest degradation was achieved with the films made at the fastest withdrawal speed (10.0 cm/min). This behavior can be explained by the higher amount of deposited material when a faster withdrawal speed was used, according to the equation proposed by Landau and Levich, which expresses that the film thickness is directly proportional to the withdrawal speed [34,35].

However, it is worth noting that a significant difference in the degradation was not detected when the withdrawal speed was increased from 7.5 to 10.0 cm/min. This result could be due to two factors: (1) further increments in the withdrawal speed after certain value not lead to an increase in the thickness or (2) further increments in the amount of deposited material after certain value are not followed by an increase in the degradation. It is worth mentioning that similar results in the photodegradation behavior were obtained using Bi_2GaNbO_7 films on 304 SS (1 layer) made at the same withdrawal speeds and therefore the previous result could be attributed mainly to the first factor.

MeO degradation over time using Bi_2GaNbO_7 films on 304 SS with different number of layers (1, 3 and 5) at a withdrawal speed of 7.5 cm/min is shown in Fig. 8.

It can be seen that the degradation increases when the number of layers was increased from 1 to 3 but a further increment to 5 layers not lead to any improvement. Undoubtedly, the enhancement in the degradation until a certain value is due to the increase in the amount of deposited material with the augment of number of layers. It is worth mentioning that similar results were obtained with the other Bi_2MNbO_7 films.

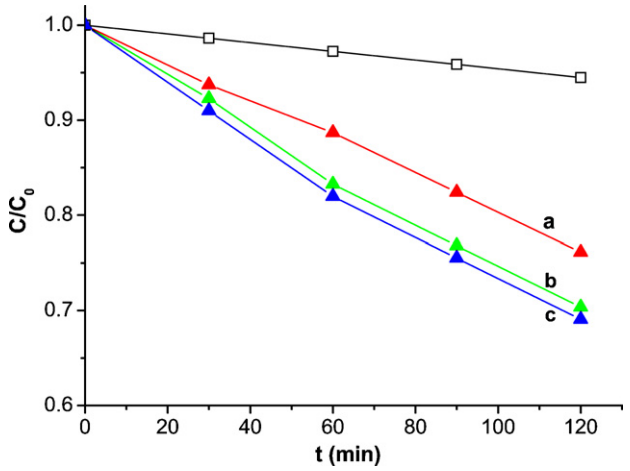

Fig. 7. Relative concentration of MeO vs. time using (▲) Bi_2GaNbO_7 films (3 layers) made at a withdrawal speed of: (a) 5.0 cm/min, (b) 7.5 cm/min, (c) 10.0 cm/min and (□) UV light (without photocatalyst).

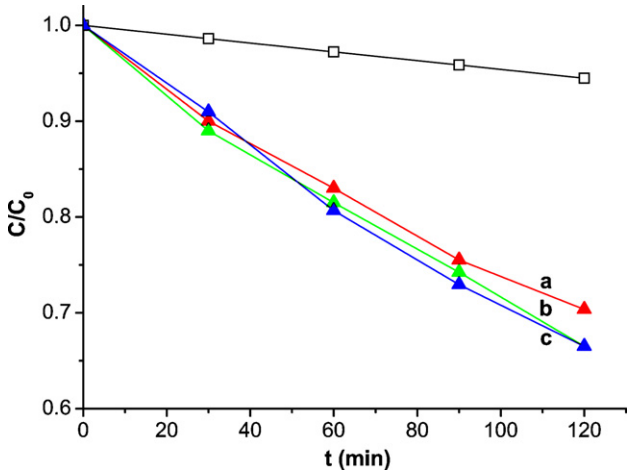

Fig. 8. Relative concentration of MeO vs. time using (▲) Bi_2GaNbO_7 films with different number of layers (7.5 cm/min): (a) 1, (b) 3, (c) 5 and (□) UV light (without photocatalyst).

All materials used in the photodegradation of MeO were subjected to several cycles of use, among which there were no significant changes in their photocatalytic performance, showing stability and resistance to the reaction conditions employed. The obtained results make further work on the subject very encouraging.

4. Conclusions

The photoactivity of Bi_2MNbO_7 films toward methyl orange degradation was higher or equivalent than that of TiO_2 films.

The Bi_2GaNbO_7 film had the higher crystallinity and the better elemental proportion according to pyrochlore-type structure, and therefore exhibited the major photocatalytic activity, expressed as highest k_{app} and lowest $t_{1/2}$.

The photodegradation of MeO increase with a faster withdrawal speed and with increases of the number of layer deposited. Degradation of MeO follows an apparent first-order kinetics as most of the pollutant, which confirm the heterogeneous catalytic character of system for diluted solution.

Acknowledgements

This work has been carried out with the financial support of COLCIENCIAS (Project 1102-332-18533, UIS Code 8422) and UIS (DIEF Ingenierías Fisicoquímicas, Project 5430). The authors thank E. Vera-López and C.A. Ortiz-Otálora (Grupo de Superficies, Electroquímica y Corrosión – GSEC, Universidad Pedagógica y Tecnológica de Colombia – UPTC) for the SEM micrographs and XRD patterns. J.A. Pedraza-Avella also thanks COLCIENCIAS for the doctoral scholarship in the frame of the program "Apoyo a la Comunidad Científica Nacional, a través de los Programas de Doctorados Nacionales, 2003".

References

[1] T. Oppenländer, Photochemical Purification of Water and Air. Advanced Oxidation Processes (AOPs): Principles, Reaction Mechanisms, Reactor Concepts, Wiley-VCH, Weinheim, 2003.
[2] S. Parsons, Advanced Oxidation Processes for Water and Wastewater Treatment, IWA Publishing, London, 2004.
[3] I.K. Konstantinou, T.A. Albanis, Appl. Catal. B: Environ. 49 (2004) 1.
[4] U.I. Gaya, A.H. Abdullah, J. Photochem. Photobiol. C: Photochem. Rev. 9 (2008) 1.
[5] K. Rajeshwar, M.E. Osugi, W. Chanmanee, C.R. Chenthamarakshan, M.V.B. Zanoni, P. Kajitvichyanukul, R. Krishnan-Ayer, J. Photochem. Photobiol. C: Photochem. Rev. 9 (2008) 171.
[6] A.G. Agrios, P. Pichat, J. Appl. Electrochem. 35 (2005) 655.
[7] A. Fujishima, X. Zhang, C. R. Chim. 9 (2006) 750.
[8] M. Kitano, M. Matsuoka, M. Ueshima, M. Anpo, Appl. Catal. A: Gen. 325 (2007) 1.
[9] X. Lin, F. Huang, W. Wang, Z. Shan, J. Shi, Dyes Pigm. 78 (2008) 39.
[10] Z. Bian, Y. Huo, Y. Zhang, J. Zhu, Y. Lu, H. Li, Appl. Catal. B: Environ. 91 (2009) 247.
[11] J.A. Byrne, B.R. Eggins, N.M.D. Brown, B. McKinney, M. Rouse, Appl. Catal. B: Environ. 17 (1998) 25.
[12] H.T. Chang, N.-M. Wu, F. Zhu, Water Res. 34 (2000) 407.
[13] S. Gelover, P. Mondragón, A. Jiménez, J. Photochem. Photobiol. A: Chem. 165 (2004) 241.
[14] S.H. Oh, D.J. Kim, S.H. Hahn, E.J. Kim, Mater. Lett. 57 (2003) 4151.
[15] C. Guillard, D. Debayle, A. Gagnaire, H. Jaffrezic, J.-M. Herrmann, Mater. Res. Bull. 39 (2004) 1445.
[16] A. Mills, G. Hill, M. Crow, S. Hodgen, J. Appl. Electrochem. 35 (2005) 641.
[17] Z. Zou, J. Ye, H. Arakawa, Chem. Phys. Lett. 333 (2001) 57.
[18] L.L. Garza-Tovar, L.M. Torres-Martínez, D. Bernal Rodríguez, R. Gómez, G. del Angel, J. Mol. Catal. A: Chem. 247 (2006) 283.
[19] J.L. Ropero-Vega, K.L. Rosas-Barrera, J.A. Pedraza-Avella, D. Laverde-Cataño, J.E. Pedraza-Rosas, M.E. Niño-Gómez, Mater. Sci. Eng. B (2010), doi:10.1016/j.mseb.2010.03.019.
[20] G.T. Brown, J.R. Darwent, J. Phys. Chem. 88 (1984) 4955.
[21] S. Al-Qaradawi, S.R. Salman, J. Photochem. Photobiol. A: Chem. 148 (2002) 161.
[22] I.M. Arabatzis, T. Stergiopoulos, M.C. Bernard, D. Labou, S.G. Neophytides, P. Falaras, Appl. Catal. B: Environ. 42 (2003) 187.
[23] Z. Zainal, L.K. Hui, M.Z. Hussein, Y.H. Taufiq-Yap, A.H. Abdullah, I. Ramli, J. Hazard. Mater. 125 (2005) 113.
[24] X. Zhang, F. Zhang, K.-Y. Chan, Mater. Chem. Phys. 97 (2006) 384.
[25] X.-G. Hou, X.-N. Gu, Y. Hu, J.-F. Zhang, A.-D. Liu, Nucl. Instrum. Meth. Phys. Res. B 251 (2006) 429.
[26] K.H. Yoon, J.S. Noh, C.H. Kwon, M. Muhammed, Mater. Chem. Phys. 95 (2006) 79.
[27] G. Balasubramanian, D.D. Dionysiou, M.T. Suidan, V. Subramanian, I. Baudin, J.-M. Laîné, J. Mater. Sci. 38 (2003) 823.
[28] Z. Zou, J. Ye, H. Arakawa, Mater. Sci. Eng. B 79 (2001) 83.
[29] S. Sokolov, E. Ortel, J. Radnik, R. Kraehnert, Thin Solid Films 518 (2009) 27.
[30] I.M. Arabatzis, S. Antonaraki, T. Stergiopoulos, A. Hiskia, E. Papaconstantinou, M.C. Bernard, P. Falaras, J. Photochem. Photobiol. A: Chem. 149 (2002) 237.
[31] J.E. Huheey, E.A. Keiter, R.L. Keiter, Química Inorgánica: Principios de estructura y reactividad, 4th ed., Oxford University Press, México, 1997, p. 120.
[32] Z. Zou, J. Ye, J. Alloys Compd. 292 (1999) 72.
[33] A. Hameed, T. Montini, V. Gombac, P. Fornasiero, J. Am. Chem. Soc. 130 (2008) 9658.
[34] C.J. Brinker, G.W. Scherer, Sol–Gel Science: The Physics and the Chemistry of Sol–Gel Processing, Academic Press, San Diego, 1990, p. 790.
[35] R.J. Candal, J. Rodriguez, G. Colón, S. Gelover, E. Vigil Santos, A. Jimenez González, M.A. Blesa, Materiales para fotocatálisis y electrofotocatálisis, in: M.A. Blesa, B. Sánchez (Eds.), Eliminación de Contaminantes por Fotocatálisis Heterogénea, CIEMAT, Madrid, 2004, p. 189.